

The Effect of Side Chains on the Reactive Rate and Surface Wettability of Pentablock Copolymers by ATRP

Aizhao Pan, Ling He, Shao Yang, Mingjun Niu

Department of Chemistry, School of Science, Xi'an Jiaotong University, Xi'an 710049, China

Correspondence to: L. He (E-mail: heling@mail.xjtu.edu.cn)

ABSTRACT: The reactive rate and surface wettability of three pentablock copolymers PDMS-*b*-(PMMA-*b*-PR)₂ (R = 3FMA, 12FMA, and MPS) obtained via ATRP for coatings are discussed. Poly(dimethylsiloxane) (PDMS) is used as difunctional macroinitiator, poly(methyl methacrylate) (PMMA) as the middle block, while poly(trifluoroethyl methacrylate) (P3FMA), poly(dodecafluoroheptyl methacrylate) (P12FMA) and poly(3-(trimethoxysilyl)propyl methacrylate) (PMPS) as the end block, respectively. Their reactive rates obtained by gas chromatography (GC) analysis indicate that 3FMA gains $8.053 \times 10^{-5} \text{ s}^{-1}$ reactive rate and 75% conversion, higher than 12FMA ($4.417 \times 10^{-5} \text{ s}^{-1}$, 35%), but MPS has $1.9389 \times 10^{-4} \text{ s}^{-1}$ reactive rate and 96% conversion. The wettability of pentablock copolymer films is characterized by water contact angles (WCA) and hexadecane contact angles (HCA). The PDMS-*b*-(PMMA-*b*-P12FMA)₂ film behaves much higher advancing and receding WAC (120° and 116°) and HCA (60° and 56°) than PDMS-*b*-(PMMA-*b*-P3FMA)₂ film (110° and 106° for WAC, 38° and 32° for HAC) because of its fluorine-rich surface (20.9 wt % F). However, PDMS-*b*-(PMMA-*b*-PMPS)₂ film obtains 8° hysteretic contact angle in WAC (114°–106°) and HAC (32°–24°) due to its higher surface roughness (138 nm). Therefore, the fluorine-rich and higher roughness surface could produce the lower water and oil wettability, but silicon-rich surface will produce lower water wettability. © 2013 Wiley Periodicals, Inc. *J. Appl. Polym. Sci.* **2014**, *131*, 40209.

KEYWORDS: coatings; films; kinetics; copolymers

Received 23 September 2013; accepted 19 November 2013

DOI: 10.1002/app.40209

INTRODUCTION

The fluorine/silicon copolymers as coating materials could provide with excellent water repellence,^{1,2} weather resistance,^{3,4} and high thermostability.^{5,6} Among the various methods for obtaining the fluorine/silicon copolymers, atom transfer radical polymerization (ATRP) for block copolymers has attracted much attention for its versatile and powerful preparation of copolymers with controllable,^{7–9} predetermined molecular weights¹⁰ and narrow molecular weight distributions.^{11–13} If the fluorinated groups are designed as the end block, it could migrate easily onto the film surface for improving the hydrophobic property.^{14,15} Whereas if the silicon-containing groups are designed as the end block, it could improve both the hydrophobic property and the adhesion to the substrate.^{16,17}

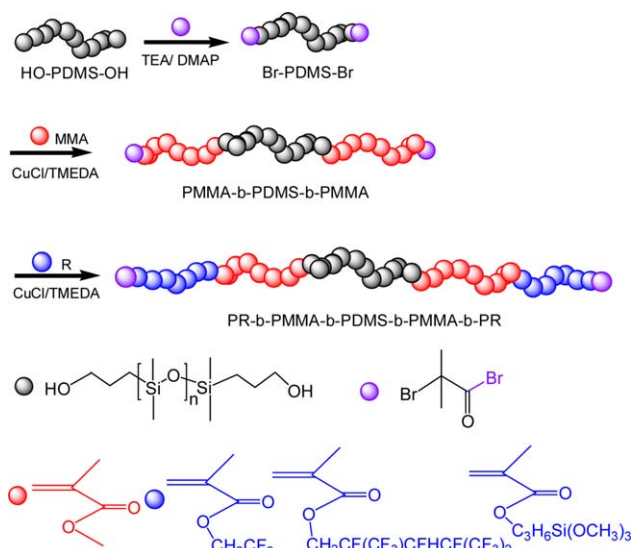
However, the key problem for the fluorine/silicon block copolymers by ATRP is the reactive rates and the conversion of monomers. It is reported that the reactive rate of ATRP for methyl acrylate would require 1 h to reach 90% conversion, but the same conversion would be reached for acrylonitrile within 1 s and for styrene within 10 h.¹⁸ Although for the different block copolymer

by the partly fluorinated monomers, the kinetic study of 2,2,2-trifluoroethyl methacrylate (3FMA), 2,2,3,3,4,4,5,5-octafluoropentyl methacrylate (8FMA), and 1,1,2,2-tetrahydroperfluorodecyl methacrylate (17FMA) in the preparation of block copolymers by ATRP are with apparent rate constants from $1.6 \times 10^{-4} \text{ s}^{-1}$ to $2.9 \times 10^{-4} \text{ s}^{-1}$.^{19,20} Therefore, the rate constant of ATRP depends mainly on the monomers. It is reported that the kinetics of diblock and triblock copolymers of 3-(trimethoxysilyl)propyl methacrylate (MPS) by ATRP follow the first-order kinetics.^{21,22} However, there is no report on the kinetics of linear pentablock fluorine/silicon copolymer in ABCBA type by ATRP.

The aim of this article is to understand the effect of fluorinated and methoxysilyl endblock on the reactive rate of three pentablock copolymers PDMS-*b*-(PMMA-*b*-PR)₂ in the linear ABCBA type, prepared by poly(dimethylsiloxane) (PDMS), poly(methyl methacrylate) (PMMA), and PR (R = poly(trifluoroethyl methacrylate) (3FMA), dodecafluoroheptyl methacrylate (12FMA) and 3-(trimethoxysilyl)propyl methacrylate (MPS)), and to realize the effect of different end blocks on the surface wettability of the films for coatings. The chemical structure and molecular weight of PDMS-*b*-(PMMA-*b*-PR)₂ are confirmed by ¹H-NMR and GPC.

Additional Supporting Information may be found in the online version of this article.

© 2013 Wiley Periodicals, Inc.



Scheme 1. The synthesis scheme of the pentablock copolymers PDMS-*b*-(PMMA-*b*-PR)₂. [Color figure can be viewed in the online issue, which is available at wileyonlinelibrary.com.]

The reactive rate of PDMS-*b*-(PMMA-*b*-PR)₂ is discussed by gas chromatography (GC) analysis. The surface wettability of films is investigated by using dynamic contact angle (DCA), X-ray photoelectron spectroscopy (XPS) for chemical element composition, and atomic force microscope (AFM) for the surface roughness.

EXPERIMENTAL

Materials

Trifluoroethyl methacrylate (CH₃CH₂=CCO₂CH₂CF₃, 3FMA, liquid), dodecafluoroheptyl methacrylate (CH₃CH₂=CCO₂CH₂CF₂CF₂CFHCF(CF₃)₂, 12FMA, liquid), and α , ω -dihydroxy terminated polydimethylsiloxane (HO-PDMS-OH, liquid, $M_n = 5000 \text{ g mol}^{-1}$) are kindly supplied by Xuojia Fluorine-Silicon Chemical Co. (China). 3-(Trimethoxysilyl)propyl methacrylate (H₂C=C(CH₃)CO₂(CH₂)₃Si(OCH₃)₃, MPS, the content exceeds 96%) provided by Silicone New material company of Wuhan University is dried over CaH₂ overnight and distilled under reduced pressure. Methyl methacrylate (MMA, 99%wt) is supplied by Chemical Industry of China. Before 3FMA, 12FMA, and MMA are used, they are rinsed with 5 wt % NaOH aqueous solution and ion-free water until the rinsed water reaches pH 7, followed by drying over calcium hydride (CaH₂, Sinopharm Chemical Reagent Co.) for 24 h and distilling under reduced pressure to remove inhibitor. 2-Bromoisobutryl bromide (BiBB), 4-(dimethylamino) pyridine (DMAP), triethylamine (TEA), and tetramethylethylenediamine (TMEDA) in

analytical purity are purchased commercially and are used as received. Cyclohexanone and tetrahydrofuran (THF) are stirred over CaH₂ for 12 h at room temperature, and distilled under reduced pressure before use. Cuprous chloride (CuCl) is purified according to the method of WhiteSides²³.

Preparation of Pentablock Copolymer PDMS-*b*-(PMMA-*b*-PR)₂

The pentablock copolymer is synthesized by two ATRP steps. First, triblock copolymer PDMS-*b*-(PMMA)₂ is prepared by macroinitiator Br-PDMS-Br²⁴ (obtained by the esterification of HO-PDMS-OH and BiBB) and MMA, as shown in Scheme 1. When CuCl and the mixture of MMA (4.88 g), Br-PDMS-Br (1.0 g), TMEDA (0.044 g), cyclohexanone (16 g) are introduced into a dry Schlenk tube under N₂ atmosphere, the reaction starts at 80°C and lasts for 24 h in an oil bath. After the left catalyst and the excess solvent are removed, the colorless solution is reprecipitated into methanol and dried in a vacuum oven overnight, the triblock copolymer Br-PMMA-PDMS-PMMA-Br is obtained. Second, the linear pentablock copolymer PDMS-*b*-(PMMA-*b*-PR)₂ is prepared by PDMS-*b*-(PMMA)₂ and MPS (3FMA or 12FMA) as in Scheme 1. When 2.61 g (20 mmol) Br-PMMA-PDMS-PMMA-Br is dissolved in 16 g cyclohexanone in a Schlenk tube, 1.22 g MPS (2.09 g 3FMA or 1.064 g 12FMA), 0.014 g CuCl and 0.033 g TMEDA are charged under N₂ atmosphere. The reaction is permitted to last for 24 h at 120°C in an oil bath. The resulting block copolymer PDMS-*b*-(PMMA-*b*-PR)₂ are obtained when the left catalyst and the excess solvent are removed. The pentablock copolymers PDMS-*b*-(PMMA-*b*-PR)₂ (R = 3FMA, 12FMA, and MPS) are synthesized with the yields of 58%, 60%, and 72%, respectively. The detail recipes of PDMS-*b*-(PMMA-*b*-PR)₂ are given in Table I.

Characterization

Nuclear Magnetic Resonance (NMR) Spectroscopy. The ¹H NMR and ¹³C NMR spectra measurement for PDMS-*b*-(PMMA-*b*-PR)₂ is performed on a Bruker AV-500 spectrometer using CDCl₃ as solvent. Tetramethylsilane (TMS) is used as the internal reference.

Gel Permeation Chromatography (GPC). The molecular weights and their distributions of the resultant copolymers are measured using a gel permeation chromatography (GPC Wyatt DAWN EOS MZ 10³+MZ 10⁴) system at 25°C. THF is used as the eluent at a flow rate of 0.5 mL min⁻¹. The molecular weight is calibrated by the polystyrene standard based on its narrower molecular weight distribution and the molecular weight of as prepared copolymers in the standard range.²⁵

Gas Chromatography (GC). GC analysis is performed with a 2010plus GC System. The GC system is equipped with an

Table I. The Detail Recipes of PDMS-*b*-(PMMA-*b*-PR)₂ and Their Molecular Weight Distribution

Block copolymers	Monomers (g)	Yield (%)	Mn (theo) ($\times 10^4$)	Mn (GPC) ($\times 10^4$)	PDI
PDMS- <i>b</i> -(PMMA- <i>b</i> -P3FMA) ₂	3FMA (2.09)	58	8.27	8.36	1.12
PDMS- <i>b</i> -(PMMA- <i>b</i> -P12FMA) ₂	12FMA (1.064)	60	7.07	9.16	1.08
PDMS- <i>b</i> -(PMMA- <i>b</i> -PMPs) ₂	MPS (1.22)	72	2.85	2.76	1.46

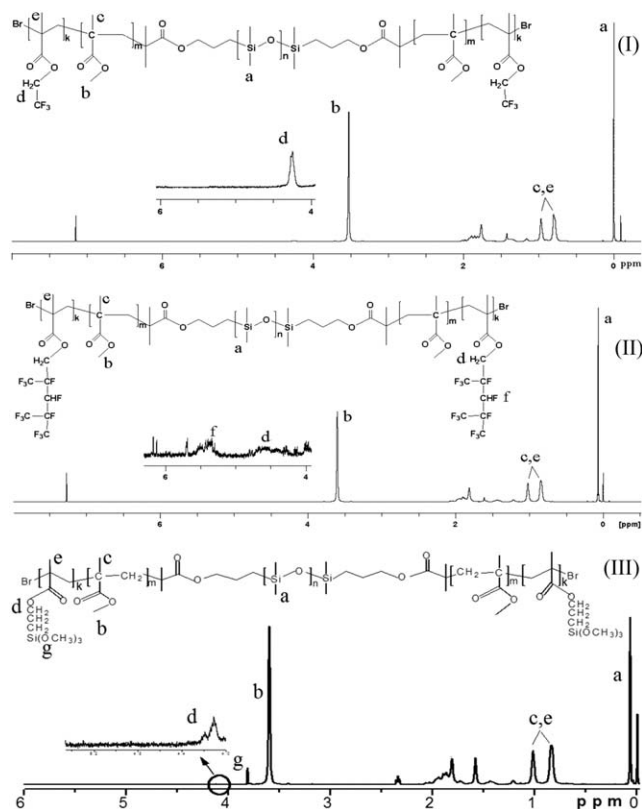


Figure 1. $^1\text{H-NMR}$ spectra of the copolymers in CDCl_3 for PDMS-*b*-(PMMA-*b*-P3FMA) $_2$ (I), PDMS-*b*-(PMMA-*b*-P12FMA) $_2$ (II) and PDMS-*b*-(PMMA-*b*-PMPS) $_2$ (III).

Hp-5MS capillary column (30 m \times 0.25 mm i.d. \times 0.25 μm) at 70°C. The carrier gas (Helium) was adjusted at a flow rate of 1.0 mL min^{-1} and split of 1:9; The injector was controlled at 200°C; All instruments were controlled by the Enhanced Chem Station (ver. 9.00.00.38) software, and the mass spectra were identified with the Wiley 138 and NIST1992 libraries. The samples are taken every each 1.5 h from Schlenk tube and precipitation in the CH_3OH solution. The upper supernate from settling

out of methanol solution is analyzed by GC to confirm the residual monomers and cyclohexanone.

Dynamic Contact Angles (DCA). The preparation of films for the obtained pentablock copolymers is casted 10 wt % solution. DCAs of distilled water and hexadecane are measured on a JY-82 contact angle goniometer (Hebei Chengde Testing Machine Co.) at room temperature. The advancing contact angle (θ_a) is obtained when contact area between the liquid droplet and the film surface is constant after increasing the droplet volume (<20 μL) twice in succession. The receding contact angle (θ_r) is obtained when the contact area is constant after decreasing the droplet volume twice in succession. The contact angle hysteresis ($\Delta\theta$) of water and hexadecane on the film surface are described by the difference between θ_a and θ_r .

X-ray Photoelectron Spectroscopy (XPS). X-ray photoelectron spectroscopy (XPS) measurements are processed on the air-exposed film surface by an AXIS ULTRA (England, KRATOS ANALYTICAL) using an Al mono K α X-ray source (1486.6 eV) operated at 150 W. The overview scans are obtained with pass energy of 160 eV and acquisition times of 220 s with a detection angle of 45.

Atomic Force Microscope (AFM). NT-MDT new Solver-Next is used to characterize the surface topographies and roughness (root-mean-square roughness) of the film samples. The measurements are taken at room temperature under 38%–42% R.H. Tip information: radius <10 nm, cantilever length 90 ± 5 nm; width 40 ± 3 nm; thickness 2.0 ± 0.5 nm, resonant frequency 330 kHz, force constant 48 N m^{-1} .

RESULTS AND DISCUSSION

Characterizing the Chemical Structure of Pentablock Copolymers

Figure 1 is $^1\text{H-NMR}$ spectra of PDMS-*b*-(PMMA-*b*-P3FMA) $_2$ (I), PDMS-*b*-(PMMA-*b*-P12FMA) $_2$ (II) and PDMS-*b*-(PMMA-*b*-PMPS) $_2$ (III). The triblock copolymer PDMS-*b*-(PMMA) $_2$ is confirmed by the typical δ_H of Si-CH $_3$ in PDMS at 0.07 ppm (d) and δ_H of O-CH $_3$ in PMMA at 3.63 ppm (b), as well as the

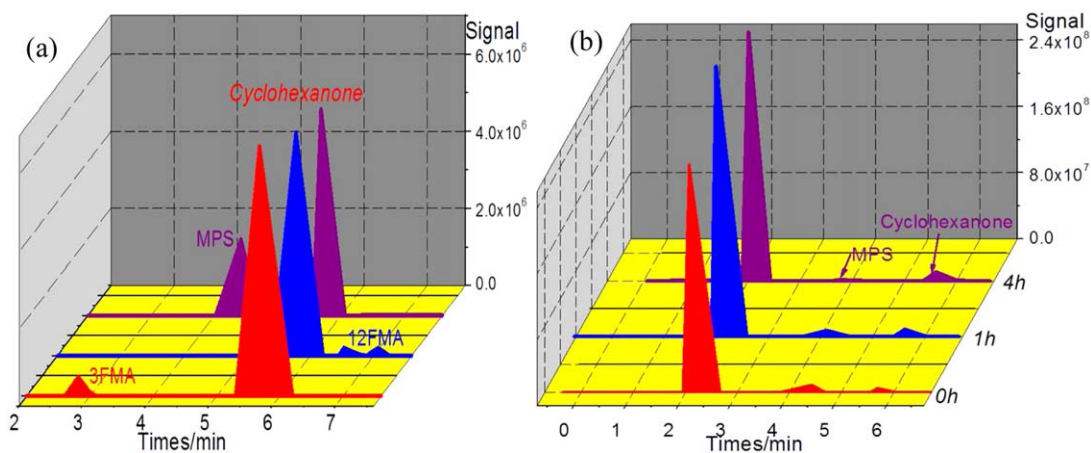


Figure 2. The peaks of possible existing in the samples in GC (a) and GC curves of sample by MPS at 0 h, 1 h, and 4 h (b). [Color figure can be viewed in the online issue, which is available at wileyonlinelibrary.com.]

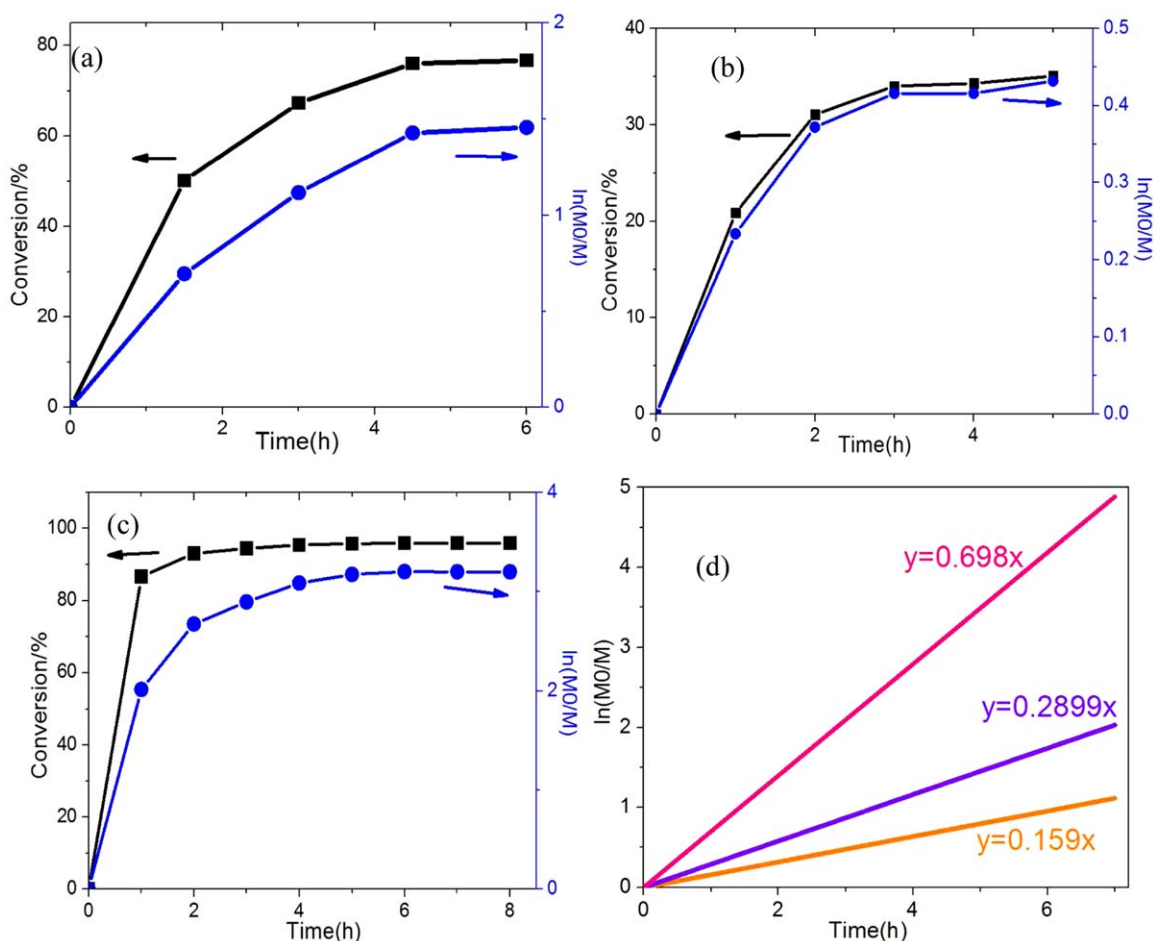


Figure 3. Time-dependence of $\ln([M_0]/[M])$ and conversion of 3FMA (a), 12FMA (b), MPS (c) in bulk at 120°C and the deduced reactive rate curves (d). [Color figure can be viewed in the online issue, which is available at wileyonlinelibrary.com.]

peaks at 1.8–2.1 ppm (c, e) for $-\text{CH}_3$ and $-\text{CH}_2$ in PMMA. The pentablock copolymers PDMS-*b*-(PMMA-*b*-PR)₂ (R = 3FMA, 12FMA and MPS) are proved by δ_H at 4.55 ppm (d) and 5.69 ppm (f) for $\text{O}-\text{CH}_2-$ and $-\text{CFH}$ in PDMS-*b*-(PMMA-*b*-P3FMA)₂ and PDMS-*b*-(PMMA-*b*-P12FMA)₂, and δ_H at 3.8 ppm (g) for $-\text{Si}(\text{OCH}_3)_3$ in PMPS segments. Furthermore, the pentablock structures of three copolymers PDMS-*b*-(PMMA-*b*-PR)₂ are also confirmed by ¹³C-NMR spectra in Supporting Information (S1).

In contrast, the GPC results for the obtained pentablock copolymers indicate the symmetric unimodal distributions with a narrow distribution in molecular weight (PDI = 1.08–1.46 in Table I). The experimental molecular weight is matched well with the theoretical values, which illustrates that the polymerization is a typical controllable ATRP. Among the three pentablock copolymers, PDMS-*b*-(PMMA-P3FMA)₂ and PDMS-*b*-(PMMA-*b*-P12FMA)₂ give the relatively narrower molecular distribution than PDMS-*b*-(PMMA-*b*-PMPS)₂. This should attribute to the free volume for the copolymer molecular in solvent by GPC measurement. Therefore, ¹H-NMR, ¹³C NMR, and GPC results are able to confirm that PDMS, PMMA, and PFMA have been polymerized via ATRP techniques into the

pentablock copolymers in ABCBA structure. It agrees well with the expected chemical structure as shown in Scheme 1.

The Reactive Rates of PDMS-*b*-(PMMA-*b*-PR)₂

The reactive rates of second ATRP for obtaining three pentablock copolymers are discussed according to the GC quantitative analysis. Considering the amount of solvent cyclohexanone (CYC) keeps constant during the second ATRP, the reaction rate of ATRP is suggested to obtain by the area ratio of the peaks between CYC and the monomers of 3FMA, 12FMA, and MPS. In this procedure, the material weight and the chromatographic peak area under the appropriate conditions are in direct proportion as follows:

$$W_M = k_M S_M, W_C = k_C S_C \quad (1)$$

Here, W_M and W_C are the monomer and CYC weight of taken samples; k_M and k_C are the mass coefficient of the monomer and CYC peaks; S_m and S_c are the peak area of the monomer and CYC in GC curves.

In the polymerization process, all the parameters of CYC are taken as constant, and the total volume of CYC (V_C) could be calculated by means of CYC weight of taken samples (W_C) and its

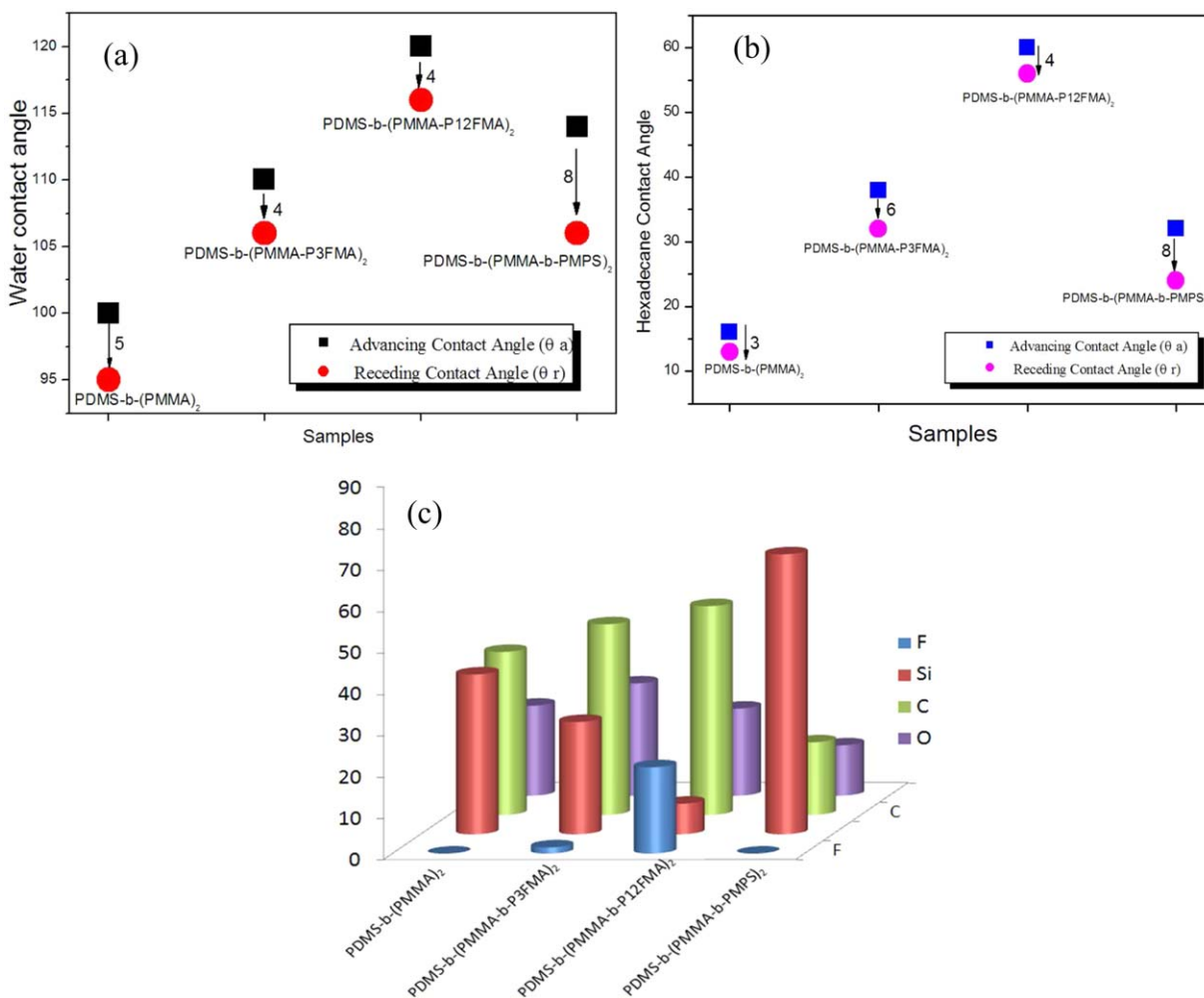


Figure 4. Dynamic contact angles for water (a), hexadecane (b) and the chemical composition (c) of pentablock copolymer films. [Color figure can be viewed in the online issue, which is available at wileyonlinelibrary.com.]

density as $V_C = W_C / \rho$. Therefore, the weight ratio between the monomer and the CYC could be described as the formula below:

$$\frac{W_M}{W_C} = \frac{k_M S_M}{k_C S_C} \quad (2)$$

$$W_M = \frac{k_M S_M}{k_C S_C} \cdot W_C = K \cdot \frac{S_M}{S_C} \cdot W_C \quad (3)$$

$$M = \frac{W_M}{M_M V_C} = \frac{\rho k_M S_M}{M_M k_C S_C} = K \frac{S_M}{S_C} \quad (4)$$

In the formula (4), M is the concentration of monomers; M_M is the molar mass of the monomers. In order to simplify the calculation, the concentration of monomer at the beginning of the reaction is defined as M_0 :

$$\ln \frac{[M_0]}{[M]} = \ln \frac{S_{M0}}{S_{C0}} \cdot \frac{S_C}{S_M} \quad (5)$$

Considering the first-order reaction for all ATRP, there must be the relationship between $\ln([M_0]/[M])$ and the reaction time as:

$$\ln \frac{[M_0]}{[M]} = kt \quad (6)$$

$$\ln \frac{S_{M0}}{S_{C0}} \cdot \frac{S_C}{S_M} = kt \quad (7)$$

Therefore, $\ln([M_0]/[M])$ could be obtained by the peak area ratio of the monomers to CYC as formula (5). Then, a variation curve of $\ln([M_0]/[M])$ to time could be used to calculate the reaction rate as formula (7) by the GC peak areas.

GC curves for three pentablock copolymers in Figure 2(a) show the retention time for 3FMA at 2.5–3 min⁻¹, for MPS at 4–4.7/min, for 12FMA at 6.5–7.2 min⁻¹ with double peaks and for CYC at 5.5–6 min⁻¹. Here, in order to identify the retention times of the monomers and CYC, all the materials existed possible in the samples have been analyzed. Figure 2(b) is an example of GC curves by PMPS as the end block at 0 h, 1 h, and 4 h, showing the decreases of peak areas with time. After being compared with the peak already calibrated by the chromatographic peaks with the unknown peaks in samples, the contents of tested materials in the sample are acquired.

Figure 3 is the distribution of $\ln([M_0]/[M])$ with time for three pentablock copolymers and their deduced reactive rates. The linear fitting is operated according to the slashes in $\ln([M_0]/$

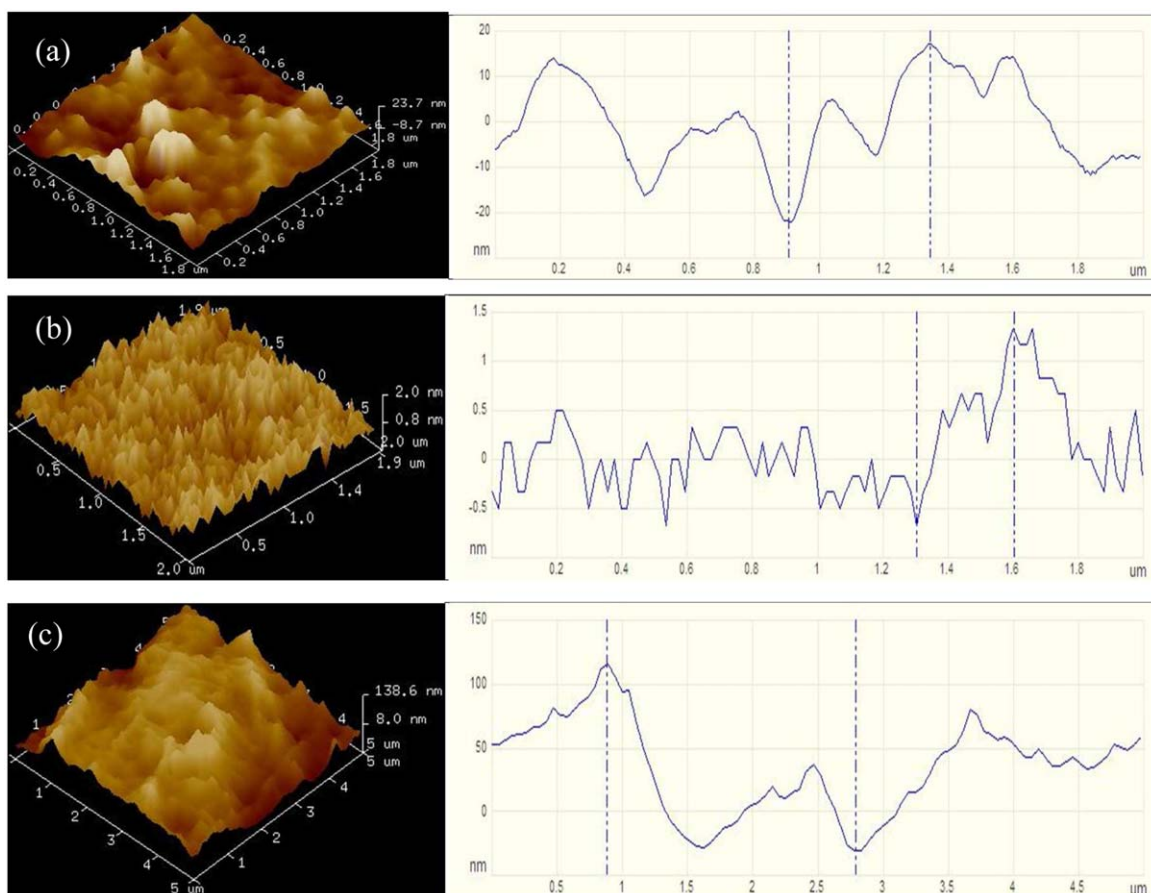


Figure 5. AFM images (3D) of PDMS-*b*-(PMMA-*b*-P3FMA)₂ (a), PDMS-*b*-(PMMA-*b*-P12FMA)₂ (b) and PDMS-*b*-(PMMA-*b*-PMPS)₂ (c) films. [Color figure can be viewed in the online issue, which is available at wileyonlinelibrary.com.]

[*M*]-*t* chart. The conversion curve for 3FMA [Figure 3(a)] shows a large increase in time and finally reaches to 75%, and the reactive rate for 3FMA is 0.2899 h^{-1} ($8.053 \times 10^{-5} \text{ s}^{-1}$) in Figure 3(d). Furthermore, in order to assure the reactive process complete thoroughly, the practical reactive time is performed within 24 h, and the same result is obtained. Figure 3(b) is the variation of $\ln([M_0]/[M])$ with time for 12FMA, which shows the reactive rate tends to zero when the reaction reaches to a critical point (about 5 h). The final reactive rate from four points (0 h, 1 h, 2 h, and 3 h) is about $0.159/\text{h}$ ($4.417 \times 10^{-5} \text{ s}^{-1}$), which is much lower than 3FMA. This difference could be explained by the segment reactivity of 3FMA and 12FMA in ATRP process. During the polymerization, the longer side chain (12FMA) moves extremely slower than the shorter side chain (3FMA), which making the kinetic energy caused by colliding could not support up the rapid reaction. Meanwhile, lower conversion for 12FMA (35%) is resulted possibly by its lower reactivity. Furthermore, when the polymerization reaches to a certain degree, the fluorinated segment begins to wind because of its weak solubility in cyclohexanone, which could farther reduce the reactivity of 12FMA as slow as $4.417 \times 10^{-5} \text{ s}^{-1}$ reactive rate. As for the reactive rate of MPS in Figure 3(c,d), it could be found that the reactive rate tends to zero after 5 h when the reaction reaches to a critical point (the same result as 12FMA), but the final reactive rate by MPS is about 0.698 h^{-1}

($1.9389 \times 10^{-4} \text{ s}^{-1}$) and the conversion rate reaches to 96%, indicating that PMS is the most active monomer used in this article, which is matched well with the previous results.²⁶

Therefore, compared with the reactive rates for 3FMA and 12FMA in Figure 3(d), it is possible to find that the longer branch side chain has the slower segment reactivity, the lower reactive rate, and the less monomer conversion. However, the reactive rate and the conversion of MPS are much higher than 3FMA and 12FMA, which demonstrates that the fluorinated monomer has the lower reactive rate and conversion. Furthermore, compared with the kinetic study for the diblock copolymer by the partly fluorinated monomers of 2,2,2-trifluoroethyl methacrylate (3FMA), 2,2,3,3,4,4,5,5-octafluoropentyl methacrylate (8FMA), and 1,1,2,2-tetrahydroperfluorodecyl methacrylate (17FMA) in the preparation of block copolymers with methyl methacrylate (MMA) by ATRP with apparent rate constants of $1.6 \times 10^{-4} \text{ s}^{-1}$ to $2.9 \times 10^{-4} \text{ s}^{-1}$, reported by Natanya et al.,³ the reactive rates for pentablock copolymers made of P3FMA ($8.053 \times 10^{-5} \text{ s}^{-1}$) and P12FMA ($4.417 \times 10^{-5} \text{ s}^{-1}$) reveal the lower reactivity.

The Surface Wettability of PDMS-*b*-(PMMA-*b*-PR)₂ Films

The dynamic contact angle (DCA) measurements of water (WCA) and hexadecane (HCA) for three pentablock copolymer films casting from THF solution are given in Figure 4. The

surface of PDMS-*b*-(PMMA-*b*-P12FMA)₂ film obtains the highest θ_a (120°) and θ_r (116°) for WCA [Figure 4(a)], as well as the highest θ_a (60°) and θ_r (56°) for HCA [Figure 4(b)], indicating its best hydrophobic and oleophobic properties. But PDMS-*b*-(PMMA-*b*-P3FMA)₂ film and PDMS-*b*-(PMMA-*b*-PMPS)₂ film give higher WCA (114°–106°) and HAC (38°–24° θ_r) than PDMS-*b*-(PMMA)₂ film (100° θ_a and 95° θ_r for WCA, 16° θ_a and 13° θ_r for HCA), showing the increasing of DCA by introducing the end blocks. Furthermore, the $\Delta\theta(=\theta_a-\theta_r)$ of 4° WCA and 6° HAC for both PDMS-*b*-(PMMA-*b*-P12FMA)₂ and PDMS-*b*-(PMMA-*b*-P3FMA)₂ films are smaller than PDMS-*b*-(PMMA-*b*-PMPS)₂ film (8° for WCA and HCA), revealing that P12FMA and P3FMA segments are favor in smaller contact angle hysteresis; and therefore, the better hydrophobic and oleophobic properties than PMPS segment. This is because the different migration of the segments chains onto the solid air interface during the film formation, which are confirmed by XPS analysis.

PDMS-*b*-(PMMA-*b*-P3FMA)₂ film could produce a silicon-rich and fluorine-poor surface at the air-polymer interface (27.2wt % Si and 1.5wt % F) [Figure 4(c)], because PDMS pendant groups are oriented at the air surface because of its greater mobility and lower surface tension than -CF₂- groups in P3FMA segments, as reported by Bilal Baradie.²⁷ However, a fluorine-rich surface with 20.9 wt % fluorine content (Supporting Information S2) is obtained for PDMS-*b*-(PMMA-*b*-P12FMA)₂ film surface, much higher than the theoretical value (11.85 wt %), because of the flexible P12FMA chains being easy to migrate onto the film surface. This migration also provides PDMS-*b*-(PMMA-*b*-P12FMA)₂ film with the highest WCA and HCA, but smaller contact angle hysteresis. Bertolucci et al. has proved that the long chain shows a well-ordered fluorocarbon surface,²⁸ but short chains are labile to surface reorganization and/or solvent adsorption. Therefore, it could be deduced that the longer chains 12FMA are able to produce fluor-rich surface, significant hydrophobic and oleophobic surface, and therefore the lower wettability. As for PDMS-*b*-(PMMA-*b*-PMPS)₂ film, Figure 4 indicates that it gives a silicon-rich surface (67.8 wt % Si) and lower wettability with 114° WCA, which reveals that the silicon-rich surface is also able to generate a lower wettability surface but a higher contact angle hysteresis.

On the contrary, the surface wettability is closely related to the surface roughness, as AFM (3D) morphology shown in Figure 5. PDMS-*b*-(PMMA-*b*-P3FMA)₂ film performs a root mean square roughness of 24 nm high [Figure 5(a)], much rough than PDMS-*b*-(PMMA-*b*-P12FMA)₂ [2.0 nm high in Figure 5(b)]. However, PDMS-*b*-(PMMA-*b*-PMPS)₂ film exhibits the largest surface roughness as 138 nm high [Figure 5(c)] and therefore a higher water contact angle (114°), although it is not a fluorine-rich surface. Therefore, the surface roughness plays an important effect more than the surface chemical composition for higher water content angle.

CONCLUSIONS

In conclusion, the effect of fluorinated end block (P3FMA, P12FMA) and methoxysilyl end block (PMPS) on the reactive

rate of linear ABCBA type pentablock copolymers PDMS-*b*-(PMMA-*b*-PR)₂ indicate that the reactive rate and conversion of 3FMA ($8.053 \times 10^{-5} \text{ s}^{-1}$, 75%) is higher than 12FMA ($4.417 \times 10^{-5} \text{ s}^{-1}$, 35%), which reveals that the longer segment of 12FMA will give the lower reactivity for pentablock copolymers, but the reactive rate and conversion for PMPS segment ($1.9389 \times 10^{-4} \text{ s}^{-1}$, 96%) are much higher than the fluorinated segment. In contrast, the effect of different end block on the surface wettability of the films reveal that the hydrophobic and oleophobic properties for PDMS-*b*-(PMMA-*b*-P12FMA)₂ film are much better than PDMS-*b*-(PMMA-*b*-P3FMA)₂ and PDMS-*b*-(PMMA-*b*-PMPS)₂ films, because PDMS-*b*-(PMMA-*b*-P12FMA)₂ film could produce a fluorine-rich top surface with 20.9wt fluorine content, but PDMS-*b*-(PMMA-*b*-P3FMA)₂ and PDMS-*b*-(PMMA-*b*-PMPS)₂ films perform silicon-rich surface. Of course, the higher surface roughness (138 nm) of PDMS-*b*-(PMMA-*b*-PMPS)₂ film is able to produce a lower wettability surface but with higher contact angle hysteresis.

ACKNOWLEDGMENTS

This work has been financially supported by the National Basic Research Program of China (973 Program, No.2012CB720904), by the National Natural Science Foundation of China (NSFC Grants No.51073126, 51373133) and by the State Administration of Cultural Heritage (20110128). The authors also wish to express their gratitude for the MOE Key Laboratory for Non-equilibrium Condensed Matter and Quantum Engineering of Xi'an Jiaotong University.

REFERENCES

1. Koda, Y.; Terashima, T.; Nomura, A.; Ouchi, M.; Sawamoto, M. *Macromolecules* **2011**, *44*, 4574.
2. Islam, M. T.; Islam, M. R.; Lim, K. T. *Polymer* **2011**, *52*, 5212.
3. Natanya, M. L.; Hansen, K. J.; Soren, H. *Eur. Polym. J.* **2007**, *43*, 255.
4. Rollings, D. E.; Tsoi, S.; Sit, J. C.; Veinot, J. G. C. *Langmuir* **2007**, *23*, 5275.
5. Ameduri, B. *Macromolecules*. **2011**, *43*, 10163.
6. Conrad, M. P. C.; Shoichet, M. S. *Polymer*. **2007**, *48*, 5233.
7. Uneyama, K. *J. Fluorine Chem.* **2008**, *129*, 550.
8. Urugmi, T.; Yamada, H.; Miyata, T. *Macromolecules* **2006**, *39*, 1890.
9. Andruzzi, L.; Hexemer, A.; Li, X. F.; Ober, C. K.; Kramer, E. J.; Galli, G. *Langmuir* **2004**, *20*, 10498.
10. Darmanin, T.; Guittard, F. *J. Am. Chem. Soc.* **2011**, *133*, 15627.
11. Braunecker, W. A.; Matyjaszewski, K. *Prog. Polym. Sci.* **2007**, *32*, 93.
12. Liang, J. Y.; He, L.; Zhao, X.; Dong, X.; Luo, H.; Li, W. *J. Mater. Chem.* **2011**, *2*, 6934.
13. Lian, K. J.; Chen, C. Q.; Liu, H.; Wang, N. X.; Yu, H. J.; Luo, Z. H. *J. Appl. Polym. Sci.* **2011**, *120*, 156.

14. Borkar, S.; Jankova, K.; Siesler, H. W.; Hvilsted, S. *Macromolecules* **2004**, *37*, 788.
15. Kyeremateng, S. O.; Henze, T.; Busse, K.; Kressler, J. *Macromolecules* **2010**, *43*, 2502.
16. Luo, Z. H.; He, T. Y.; Yu, H. J.; Dai, L. Z. *Macromol. React. Eng.* **2008**, *2*, 398.
17. Han, M.; Rahman, M. S.; Lee, J. S.; Khim, D.; Kim, D. Y.; Park, J. W. *Chem. Mater.* **2010**, *23*, 3517.
18. Matyjaszewski, K. *Macromolecules* **2012**, *45*, 4015.
19. Hansen, N. M. L.; Haddleton, D. M.; Hvilsted, S. *J. Polym. Sci. Part A: Polym. Chem.* **2007**, *45*, 5770.
20. Hansen, N. M. L.; Gerstenberg, M.; Haddleton, D. M.; Hvilsted, S. *J. Polym. Sci. Part A: Polym. Chem.* **2008**, *45*, 8097.
21. Luo, Z. H.; He, T. *React. Funct. Polym.* **2008**, *68*, 931.
22. Xiong, M.; Zhang, K.; Chen, Y. *Eur. Polym. J.* **2008**, *44*, 3835.
23. Whitesides, G. M.; Sadowski, J. S.; Lilburn, J. *J. Am. Chem. Soc.* **1973**, *96*, 2829.
24. Luo, Z. H.; Yu, H. J.; He, T. Y. *J Appl Polym Sci* **2008**, *108*, 1201.
25. Semsarzadeh, M. A.; Abdollahi, M. *J Appl Polym Sci* **2012**, *123*, 2423.
26. Du, J.; Chen, Y. *Macromolecules* **2004**, *37*, 6322.
27. Baradie, B.; Shoichet, M. S. *Macromolecules* **2005**, *38*, 5560.
28. Bertolucci, M.; Galli, G.; Chiellini, E. *Macromolecules* **2004**, *37*, 3666.